Colloids and Surfaces A: Physicochemical and Engineering Aspects 690 (2024) 133775

Contents lists available at ScienceDirect

Colloids and Surfaces A: Physicochemical and Engineering Aspects

journal homepage: www.elsevier.com/locate/colsurfa

Aqueous dispersions of oleic acid nanodroplets for thymol encapsulation

Paula Gutiérrez-González [a,1], Laura Fernández-Peña [b], Alejandro Lucia [c], Francisco Ortega [a,d], Ramón G. Rubio [a,d], Eduardo Guzmán [a,d,*]

[a] Departamento de Química Física, Facultad de Ciencias Químicas, Universidad Complutense de Madrid, Plaza de las Ciencias 2, Ciudad Universitaria, Madrid 28040, Spain
[b] Centro de Espectroscopia y Correlación, C.A.I. de Técnicas Químicas, Universidad Complutense de Madrid, Plaza de las Ciencias 2, Ciudad Universitaria, Madrid 28040, Spain
[c] Grupo de Manejo Integrado y Bioecología de Artrópodos Dulceacuícolas (MIyBAD) -Instituto de Ecología y Desarrollo Sustentable (INEDES, CONICET-UNLu), Ruta 5 y Avenida Constitución, Luján, Buenos Aires 6700, Argentina
[d] Instituto Pluridisciplinar, Universidad Complutense de Madrid, Paseo Juan XXIII 1, Ciudad Universitaria, Madrid 28040, Spain

GRAPHICAL ABSTRACT

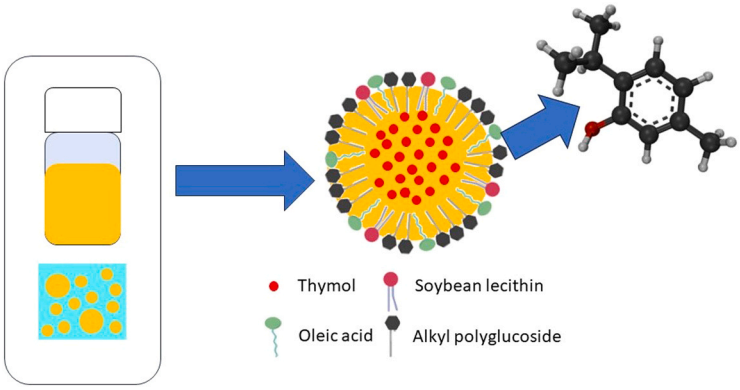

ARTICLE INFO

Keywords:
Dispersion
Emulsions
Encapsulation
Nanodroplets
Thymol

ABSTRACT

This study focuses on the use of oleic acid to disperse thymol as nanodroplets, stabilized by a mixture of alkylpolyglucoside and lecithin, in an aqueous environment. This approach aims to develop innovative platforms for the encapsulation and release of poorly water-soluble molecules such as thymol, useful for drug delivery and insecticide systems. The results highlight the critical role of controlling the content and concentration of the oil phase (thymol-oleic acid mixture) in achieving optimal thymol dispersion and nanodispersion stability. The interplay between the ability of oleic acid to inhibit thymol crystallization and the maximum dispersible oil amount is crucial. It affects the dispersion of thymol within the nanodroplets and influences coalescence and Ostwald ripening phenomena. The balance between oleic acid and thymol content is key: while oleic acid

* Corresponding author at: Departamento de Química Física, Facultad de Ciencias Químicas, Universidad Complutense de Madrid, Plaza de las Ciencias 2, Ciudad Universitaria, Madrid 28040, Spain.
E-mail address: eduardogs@quim.ucm.es (E. Guzmán).
[1] Current Address: Departamento de Química en Ciencias Farmacéuticas, Facultad de Farmacia, Universidad Complutense de Madrid. Plaza de Ramón y Cajal s/n, Ciudad Universitaria, 28040 Madrid, Spain.

https://doi.org/10.1016/j.colsurfa.2024.133775
Received 22 January 2024; Received in revised form 1 March 2024; Accepted 18 March 2024
Available online 21 March 2024

stabilizes dispersions, higher thymol content increases droplet size, potentially triggering destabilization. The uneven distribution of thymol within the droplets, revealed by fluorescence spectroscopy, suggests that up to three different chemical environments exist. This investigation may pave the way for the development of efficient platforms to improve access to biologically relevant, poorly soluble molecules.

1. Introduction

The encapsulation of various active ingredients of hydrophobic nature in oil nanodroplets has gained significant attention due to the unique physicochemical properties of this type of systems. This method provides protection and stability to the encapsulated molecules, and sometimes the possibility of a controlled and targeted release of active molecules [1]. This makes it possible to increase the bioavailability of poorly soluble ingredients, improve their distribution, and protect them from physicochemical processes and/or agents that could lead to their degradation Furthermore, this increases the shelf life of highly labile compounds [2].

Essential oils and their individual components encompass a wide range of biological activities, e.g., antioxidant, anti-inflammatory, antimicrobial, antifungal, or insecticidal, that have fueled their historical use as food preservatives and medicinal agents for centuries [3,4]. In addition, interest in this type of molecules has grown in recent years due to their potential applications in various industries, including cosmetics, food, and pharmaceuticals [2,5]. However, the development of the applications of this type of molecules requires preserving their chemical and biological properties for a relatively long time. In fact, the application of essential oils and their individual components can be limited due to their chemical and biological instability, strong aroma, high volatility, and risk of degradation upon exposure to heat, humidity, light, or oxygen [6,7]. Therefore, seeking for strategies to prevent the degradation of the active molecules is a key challenge for exploiting their physico-chemical properties industrially.

Encapsulation of essential oils and their individual component is a promising alternative to increase the potential uses and efficacy of essential oils in food preservation, pharmaceuticals, and other industries [8,9]. To date, there is a wide range of methods available for encapsulating essential oils and their individual components [10–14]. Among these encapsulation approaches, their encapsulation as oily nanodroplets dispersed in water to form nano- or microemulsions has gained importance in recent years. This approach provides a suitable environment to ensure good dispersion of the hydrophobic molecules in the aqueous environment and protects them from degradation and oxidation, thus avoiding deterioration of the active molecules and improving their stability during storage and transport [2,15–17].

This work explores the potential application of nanodroplets of oleic acid, stabilized by a mixture of two surfactants (an alkylpolyglucoside and soybean lecithin), as carriers for thymol. Thymol is a natural monoterpenoid phenol derivative of p-cymene found in the oil of thyme, presenting a pleasant aromatic odor and strong antiseptic properties [18,19]. However, the exploitation of their biological properties is not always easy because of their limited solubility in water. In fact, thymol is a white crystalline hydrophobic solid (melting point around 50ºC) [20], and its dispersion within the interior of oleic acid nanodroplets can contribute to increase its apparent solubility in water. This may allow for higher concentrations of thymol to be delivered, potentially leading to enhanced bioactivity [21–23]. Moreover, the use of soybean lecithin and oleic acid in the preparation of the dispersions can contribute to facilitate the penetration of the encapsulated active ingredients through biological membranes, which can be very interesting in the potential application of this type of colloidal dispersions in drug delivery, food industry, or cosmetics [24,25]. However, while lecithin offers significant advantages for the internalization of drug-loaded nanodroplets in human contact applications, its inherent ability to stabilize emulsions when used alone is somewhat limited. Consequently, the combination of lecithin with other surfactants may become an effective strategy to harness the favorable biological properties of lecithin in formulation [26]. To improve stability and optimize performance, an alkylpolyglucoside was chosen to complement lecithin due to its favorable penetration ability and low toxicity profile. This combination not only addresses the stabilization challenges associated with lecithin alone, but also capitalizes on the desirable properties of both components for an improved and well-balanced formulation [27].

2. Materials and methods

2.1. Chemicals

Oleic acid of >99% purity was purchased from Sigma-Aldrich (St. Louis, MO, USA) and used as the carrier oil for dispersion preparation. Thymol (at least 98.5% purity, 2-isopropyl-5-methylphenol) was also purchased from Sigma-Aldrich (St. Louis, MO, USA). Nanodroplet stabilization in aqueous medium was achieved using mixtures of two different surfactants. These mixtures consisted of different weight fractions of alkylpolyglucoside (APG), marketed as Oramix GC-110 (a 50:50 molar combination of caprylyl glucoside and capryl glucoside), supplied by Safic-Alcan (Barcelona, Spain), and soybean lecithin (SL, 2-linoleoyl-1-palmitoyl-sn-glycero-3-phosphocholine) of >90% purity, obtained from Alfa Aesar (Haverhill, KS, USA).

For dispersion preparation, ultrapure deionized water (Milli-Q quality), with resistivity >18 MΩ•cm, and a total organic content of <6 ppm, was obtained using the AquaMAX™-Ultra 370 Series multicartridge purification system from Young Lin Instrument Co., Ltd. (Gyeonggi-do, South Korea).

2.2. Nanodroplet dispersion preparation

Three series of emulsions were prepared in which the total composition of the surfactant mixture (APG:SL) used to stabilize the nanodroplets was fixed at 30% of the total mass of the dispersion and the APG:SL ratio was set at 8:1. The choice of this composition was made following the work by Fernández-Peña et al. [28] who showed that at this composition stable dispersions of oleic acid in water could be obtained with the surfactant mixture used. Furthermore, this composition is far from the phase separation boundaries, suggesting that the solubilization of a hydrophobic substance within the oleic acid nanodroplets would not destabilize the dispersions. The variation among the series studied was the percentage of the oil phase consisting of oleic acid and the dispersed molecule (thymol). This resulted in an oily phase weight fraction varying between 0.03 and 0.05 of the total mass of the dispersion. As a result, the weight percentage of the liquid phase remained constant at 70% of the dispersion mass in all the cases studied, allowing the study of the effect of the variation of the oil/water ratio on the stability of the emulsions and the efficiency of the thymol distribution in the nanodroplets.

The dispersions were prepared by weighing (which allows one to express the dispersion composition in weight fraction of the different components) in tubular vials, following a specific order of component addition. First, the appropriate amount of oleic acid was added, followed by the required amount of thymol since these two components form the oily phase and prior solubilization of the active ingredient in this phase is necessary. The required amount of APG was then added, followed by that of lecithin. To ensure perfect solubilization of the lecithin, the mixture was vortexed for 30 seconds before the addition of Milli-Q

water. To ensure proper lecithin solubilization and to obtain a homogeneous mixture, the samples were mechanically stirred with a magnetic stirrer (1200 rpm) at a temperature of 50ºC. Once the homogeneity of the dispersions was assured, they were allowed to cool and stabilize for 24 hours before classification and characterization. All tests were performed at 25.0 ± 0.1ºC.

2.3. Experimental techniques

The average size of the oil nanodroplets dispersed in water was evaluated in terms of the apparent hydrodynamic radius, R_H^{app}, obtained by dynamic light scattering (DLS). For these experiments, a Zetasizer Nano ZS (Malvern Instrument Ltd., Malvern UK) equipped with a He-Ne laser (wavelength 632 nm) and operating in a quasi-backscattering configuration (scattering angle 173º) was used. Prior to the measurements, the samples were filtered through an inert filter with a pore size of 0.45 μm (Fisher Scientific (Hampton, NH, USA), and introduced into an optical quartz cuvette (Hellma GmbH und Co. KG, Müllheim, Germany). The data were analyzed using the CONTIN method. Further details on DLS experiments can be found in previous publications [28–30].

Conductivity measurements of the microemulsions were performed with a Methrom 856 conductimeter (Methrom AG, Herisau, Switzerland) using a 5-ring platinum conductivity cell (Methrom AG, Herisau, Switzerland). The accuracy and reproducibility of the obtained conductivities were always better than 5%.

Studies on the solubilization of thymol in oleic acid nanodroplets were performed by fluorescence spectroscopy using an FP-6500 fluorescence spectrophotometer (Jasco Inc., Easton, USA). A fixed excitation wavelength of 280 nm was selected. The choice of this wavelength for excitation was made based on previous studies found in the literature where it was indicated that, according to the optical properties of thymol, the use of this wavelength would allow the highest excitation efficiency [31].

3. Results and discussion

3.1. Determination of partial pseudo-ternary phase diagram

The determination of the pseudo-ternary phase diagram (varying the composition of water, oleic acid and thymol while keeping the composition of APG and SL constant) within the compositional region of interest is the first step in the study of multicomponent systems such as the considered here. The phase diagram makes it possible to delineate the compositional regions corresponding to the formation of stable dispersions and to identify compositions in which phase separation occurs. Furthermore, it facilitates the determination of the type of dispersions formed by varying the proportions of different components, thus allowing the characterization of the stability region of the system. It should be noted that the system analyzed is composed of five components: water, oleic acid, thymol, lecithin and APG. This results in an extremely complex phase diagram, even if pressure and temperature (25ºC) are constant, as in the present case. However, as discussed above, the APG:lecithin ratio (8:1) and the weight fraction of the surfactant mixture (0.30) were kept constants for all samples, simplifying the phase diagram to a slice of the full phase diagram, where the only variables are the concentrations of oleic acid, water, and thymol. The determination of the type of system for each composition studied was made by visual inspection, classifying the obtained dispersions into three groups: (i) transparent dispersions of nanodroplets in water and fluidity; (ii) turbid dispersions, possibly emulsions or nanoemulsions; and (iii) phase-separated systems. Consequently, the compositional region corresponding to the formation of transparent dispersions, the focus of this study, is surrounded by other regions where turbid dispersions and phase-separated systems are formed (multiphase region). The pseudo-ternary phase diagram for the studied system (water/oleic acid/thymol) is shown in Fig. 1.

As can be seen in the phase diagram obtained, the formation of transparent dispersions of nanodroplets is possible for weight fractions of oleic acid and thymol in the whole dispersion ranging 0–0.05 and 0–0.03, respectively. As the composition moves away from the indicated values, the coalescence and Ostwald ripening between the droplets increase their average size, which pushes the system to a region where turbid dispersions of nanodroplets or directly phase separated samples are obtained.

The results show that for a fixed water/surfactant/oil composition, the variation of the composition of the oil phase present a critical impact on the stability of the dispersions. In particular, for the here studied case the increase in the thymol concentration in the oil phase at a fixed weight fraction of the oil phase appears as a critical parameter for the stability of the nanodroplet dispersions. This is clearly visible in the two images in Fig. 2, which show the aspect of samples with different oleic acid/thymol concentration ratios for two different oil weight fractions (0.04 and 0.05).

The two images show that as the thymol content increases and the oleic acid content decreases, while the total oil phase content remains constant, the system moves away from the stability region towards phase separation. This is evident by the transition from yellowish/orange translucent dispersions to opaquer dispersions or phase separated mixtures, with the latter characterized by the appearance of a second phase, as the thymol content is increased. In addition, the destabilization of the emulsions occurs for lower fractions of thymol in the oil phase as the weight fraction of the amount of oil in the dispersion is increased.

The decrease in the dispersion stability with the increase of thymol content on the oil phase can be understood considering the need of a minimal oleic acid/thymol compositional ratio to ensure the dispersion of solid thymol within the oil phase. Thus, considering the set of samples with total oil weight fraction of 0.04, the emergence of phase separation corresponds to an oleic acid/thymol compositional ratio in the oil phase of 1/3. This means that the maximum thymol amount that can be dispersed corresponds to a weight fraction just below of 0.03 referred to the whole dispersion. Similarly, when the weight fraction of oil phase is

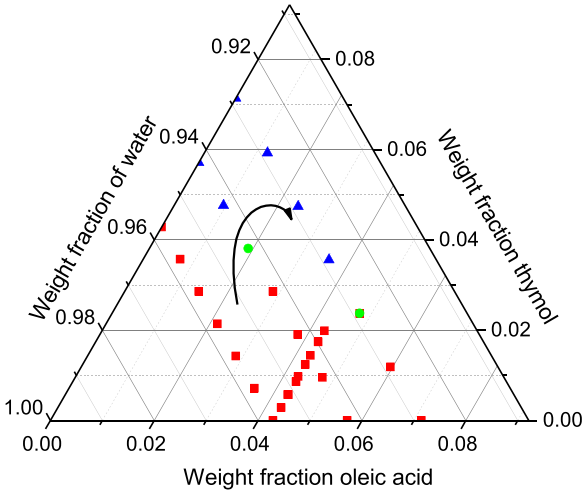

Fig. 1. Pseudo-ternary phase diagram representing a cut of the whole phase diagram obtained at 25 °C for the dispersion obtained (concentration of surfactant mixture 30%w/w and 8:1 APG:SL ratio). The phase change of the transparent dispersions to turbid dispersion and phase separated systems is evidenced with an arrow in the phase diagram. The different nature of the dispersions obtained are evidenced with different symbols: transparent dispersions (■), turbid dispersions (●) and phase separated mixtures (▲). Notice that axes represent the weight fraction of the components, with the composition of the ternary mixture, water/oleic acid/thymol, referred to unity. The arrow represents the transition from transparent dispersions to phase separation.

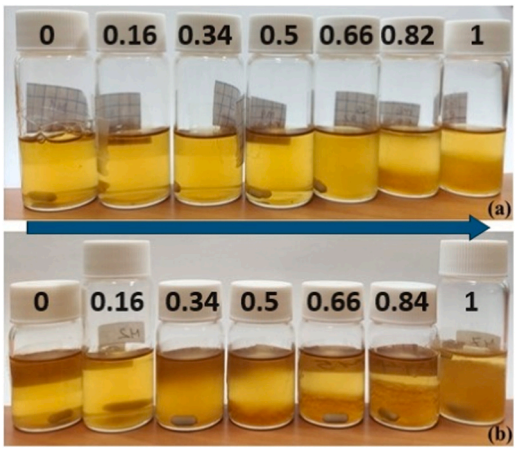

Fig. 2. Photos of the dispersions of oil-in-water with values of the weight fraction of the oil phase of 0.04 (a) and 0.05 (b), stabilized by a total concentration of the surfactant mixture of 30%w/w, with an APG:SL ratio 8:1, and different composition of the oil phase (different oleic acid/thymol concentration ratio). The arrow indicates the direction in which the concentration of thymol is increasing in the oil phase, and the labels on the top of each vial indicate the thymol weight fraction in the oil phase.

increased up to 0.05, the maximum dispersion of thymol corresponds to a compositional ratio in the oil phase of 1/2, which is equivalent to a weight fraction 0.025 referred to the whole dispersion. This behavior can be only understood considering that thymol is initially a solid that during the preparation of the dispersion melts and mixes with the oleic acid, and therefore it is plausible that oleic acid can contribute to ensure if dispersion, retarding its crystallization in agreement with the scenario proposed by Doost et al. [32]. However, this alone is not enough to explain the emergence of the phase separation at lower thymol concentrations when the total oil content is increased, because the results show that phase separation appears at higher concentrations of oleic acid when the weight fraction of the oil phase is increased, which is contradictory with the above discussion. In fact, considering the retarding effect of the solvent (oleic acid) in the crystallization of thymol, one could expect that the emergence of instability of the dispersions appeared at higher values of the thymol content as weight fraction increase, i.e., it should appear at lower values of the oleic acid/thymol compositional ratio. This suggests the existence of a second concurrent process operating in the opposite direction to contribute to the dispersion destabilization. This second process may be associated with the reduction of ratio surfactant/oil phase compositional ratio. Thus, the increase in the weight fraction of the oil phase whereas the weight fraction of the surfactant mixture is maintained as a constant leads to a situation in which the amount of surfactant is not high enough

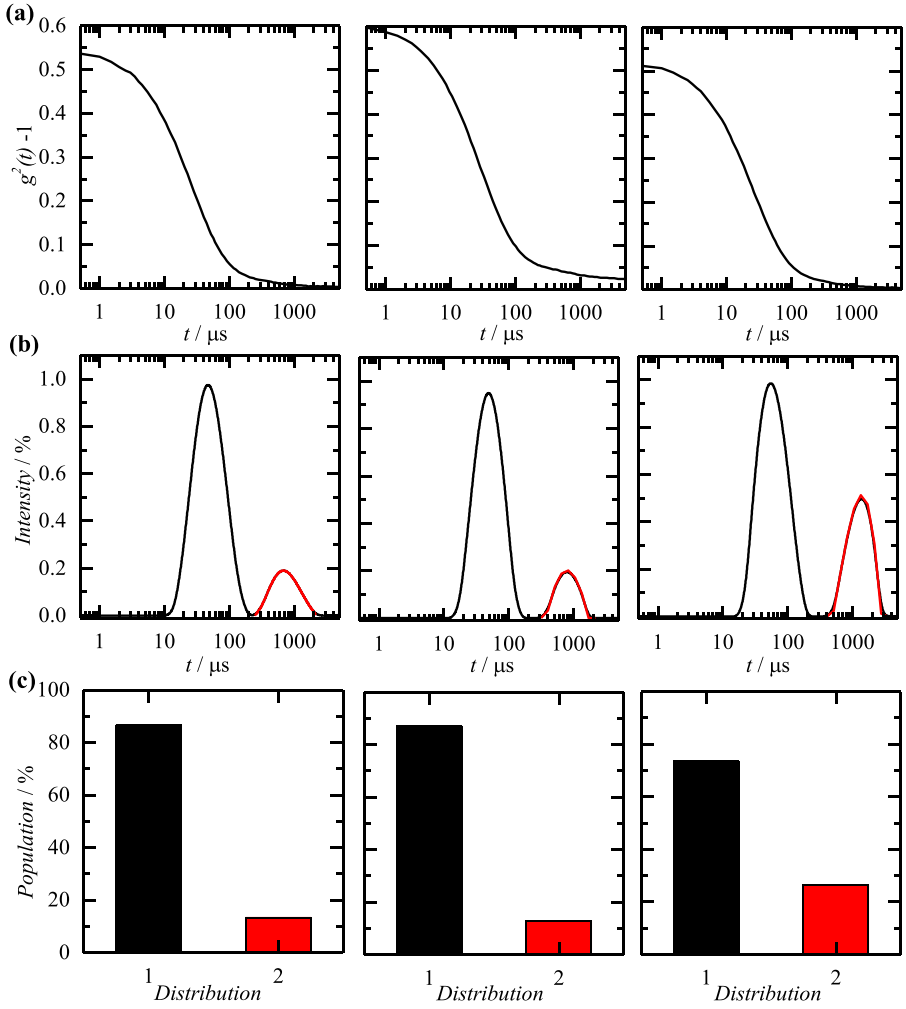

Fig. 3. DLS results for nanodroplet dispersions containing an oil phase with the same oleic acid/thymol compositional ratio (0.83:0.17) and different total oil weight fraction in the dispersion (starting from 0.03% on the left, 0.04% in the middle and 0.05% on the right). (a) intensity auto-correlation functions, (b) intensity-relaxation time distributions obtained from the analysis of the auto-correlation functions of intensities, and (c) percentage of population in each mode appearing in the distributions of intensities.

to form a dense shell to prevent the destabilization events. This favors the coalescence and Ostwald ripening of the droplet, counteracting in part the retarding effect of the oleic acid to hinder the recrystallization of the thymol.

3.2. Evaluation of the nanodroplet size

Using DLS measurements, it was possible to estimate the size of the nanodroplets dispersed in the aqueous phase in terms of their apparent hydrodynamic radius, R_H^{app}. To this aim, it is necessary to carry out an analysis of the autocorrelation functions of the intensities obtained experimentally for each of the dispersions studied (it should be noted that the use of DLS is only possible for transparent samples, therefore cloudy samples or phase separated samples have been discarded). Fig. 3 shows a series of intensity auto-correlation functions and the corresponding intensity distributions obtained from their analysis. It also shows the percentage of each of the populations corresponding to the different dynamic modes that appear in the intensity distributions for the different nanodroplet dispersions studied.

The results corresponding to the intensity autocorrelation functions shown in Fig. 3a indicate that the nanodroplet dynamics is characterized by a bimodal intensity autocorrelation function, regardless of the composition analyzed. In all cases, the decay of the fast mode is similar, while the decay of the slow mode occurs at longer times as the oil phase content increases, which can be attributed to an increase in the average droplet size. The formation of larger droplets with increasing oil phase content is qualitatively consistent with the increase in the tendency of nanodispersions to undergo phase separation with increasing oil phase content discussed above. The above scenario is most clearly seen in Fig. 3b, where the intensity distributions extracted from the analysis of the intensity autocorrelation functions are plotted.

The results point out the appearance of two distributions of relaxation times for the dispersions, i.e., two populations. This is consistent with the bimodal nature of the intensity autocorrelation functions, with the second distribution appearing at longer times, i.e., larger characteristics sizes, as the oil phase content increases. This is related to the increase in the apparent hydrodynamic radius of the droplets as the percentage of total oil phase increases. This increase in apparent hydrodynamic radius could be attributed to an increase in droplet instability due to a decrease in the amount of APG:SL mixture relative to the amount of oil, which favors coalescence and Ostwald ripening phenomena and thus droplet growth. The latter can be easily understood from the analysis of the results in Fig. 3c, where the percentage corresponding to the population of each mode is given as a function of the total weight percentage of oil phase. The results show that for the lowest weight fraction of oil phase (0.03–0.04) there is hardly any significant change in the contribution of the mode, which decays at longer times. However, as the total oil phase content increases up to a weight fraction of 0.05, the importance of the mode with long decay time increases, which is related to an increase in droplet size and the proximity of the dispersion to the entrance of the phase separation region.

Fig. 4 provides a detailed examination of the average droplet size within the investigated dispersions. This figure illustrates the relationship between the average apparent hydrodynamic radius and the weight fraction of thymol, denoted as χ_{thymol}, referred to the total composition of the oil phase. The average hydrodynamic radii corresponding to distinct droplet populations were determined using the Stokes-Einstein relationship, which establishes a connection between the average diffusion coefficient (D) and the apparent hydrodynamic radius (R_H^{app}) according to $D = k_B T/6\pi\eta R_H^{app}$. Here, k_B and T represent the Boltzmann constant and the absolute temperature, respectively, while η denotes the viscosity of the continuous medium. The average diffusion coefficient is inversely proportional to the characteristic relaxation time of the corresponding process observed in the intensity auto-correlation function, with the square of the scattering wavevector being the proportionality constant [33]. It is essential to note that the reported values for hydrodynamic radius and diffusion coefficient are considered averages. These calculations rely on the characteristic times of the relaxation processes observed in the intensity auto-correlation function. This approach contrasts with using the entire time distribution, which results in a distribution of diffusion coefficients and hydrodynamic radii similar to those depicted for relaxation times in Fig. 3b. The size of this distribution is represented in Fig. 4 by its width at half-height, presented as an error bar. Based on the about, it is possible to obtain a comprehensive understanding of the droplet sizes within the studied dispersions, taking into account the inherent variability in the measured parameters.

As it can be observed, the dispersions obtained are polydisperse, as droplets of two different average sizes appear, in agreement with the appearance of two populations discussed in Fig. 3. The smaller droplet sizes have an $R_H^{app} \sim 5$–10 nm, that remains relatively constant for dispersions with different total weight fractions of the oil phase and different thymol contents within the oil phase. However, the trend is not the same for the larger droplets associated with the slow relaxation mode in the intensity autocorrelation functions, where there is a noticeable increase in size with increasing oil phase content. As mentioned above, this may be due to the fact that the composition of the surfactant mixture (APG:lecithin 8:1) and its weight fraction remain constant for all dispersion studied, so that at small weight fractions of oil

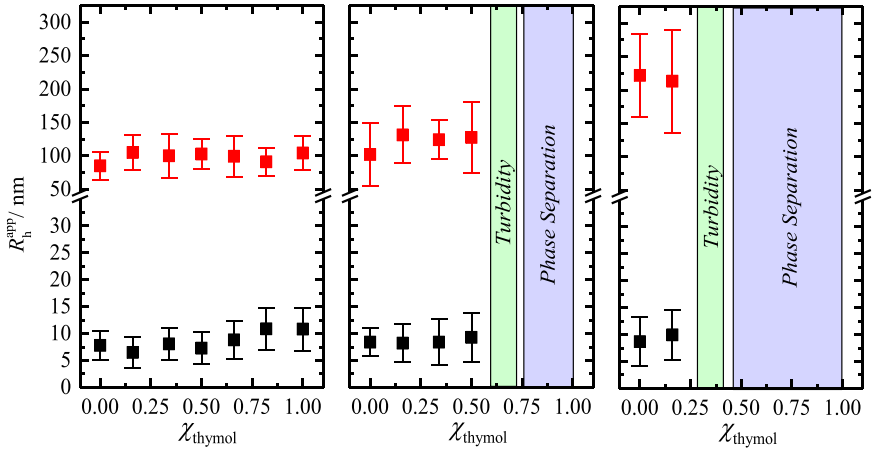

Fig. 4. Average R_H^{app} for the different types of droplets in the dispersion as a function of the weight fraction of thymol in the oil phase for dispersions with different total oil phase concentrations (oleic acid+thymol, starting on the left with 0.03, in the middle with 0.04 and on the right with 0.05). Note that the plots show the compositions corresponding to turbid dispersions and phase separated mixtures. The error bars represent the width at half-height of the apparent hydrodynamic radius distributions.

phase (0.03–0.04), the surfactant allows the formation of a dense shell at the droplet/aqueous phase interface, thus minimizing coalescence and Ostwald ripening and providing higher stability to the small droplets in the microemulsions. This limits the increase in the number of large droplets and inhibits, at least partially, their growth. However, as the amount of oil increases, the concentration of the surfactant mixture is not enough to form a sufficiently dense film at the droplet/aqueous phase interface that ensure the dispersion of the whole oil volume and therefore the importance of the destabilization phenomena increases, leading to an increase in droplet size.

The results show that the average hydrodynamic radius of the largest droplets doubles when moving from dispersions with oil weight fractions in the range of 0.03–0.04 to dispersions with oil weight fractions of about 0.05. In addition to the effect associated with increasing the weight fraction of the oil phase on droplet stability, the DLS results also show that as the concentration of thymol in the dispersion increases, droplet destabilization occurs, slightly increasing the size of the larger droplets, and that phase separation occurs at lower thymol concentrations with increasing total oil phase content.

3.3. Ionic conductimetry measurements: a tool for evaluating the organization of molecules within the nanodroplets

Ionic conductivity measurements in dispersions provide information on the distribution of the different species in the system, and it is expected to be a property that is particularly sensitive to both the weight fraction of the dispersed phase of the dispersion and its composition, especially if some of the species in the oil phase can be selectively organized into the interfacial region of the droplets. Fig. 5 shows the dependence of the ionic conductivity, κ, both as a function of the variation of the weight fraction of thymol in the oil phase for dispersions with a constant content of oil phase (Fig. 5a), and as a function of the total weight fraction of the oil phase for dispersions where the oleic acid/thymol compositional ratio is kept constant.

The ionic conductivity results shown in Fig. 5a indicate that the ionic conductivity values decrease as the thymol content in the oil phase increases. This can be understood considering that the oleic acid can be distributed between the droplet/aqueous phase interface and the core of the nanodroplet. Therefore, as the amount of thymol increases it replaces oleic acid in the oil phase, resulting in fewer oleic acid molecules with their dissociated carboxylate group exposed to the aqueous phase. This contributes to the decrease in conductivity due to the reduction in free ions. On the other hand, the conductivity values decrease as the total oil phase content increases, as shown in Fig. 5b, which is equivalent to say that the conductivity decreases as the water content increases. This can be explained by the assumption that the conductivity is due to

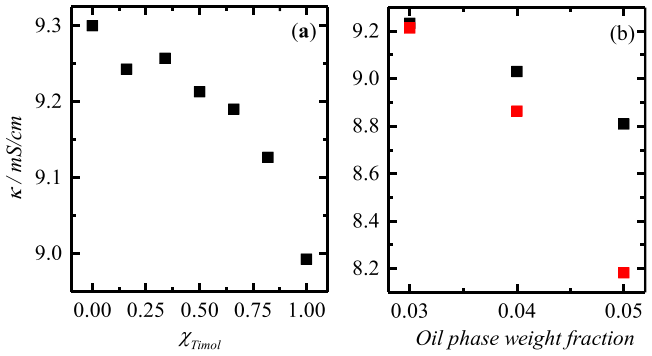

Fig. 5. Ionic conductivity measurements for oil nanodroplet dispersions. (a) Dependence of the ionic conductivity on the weight fraction of thymol in the oil phase for dispersions with a fixed weight fraction of oil phase (0.03) and (b) ionic conductivity dependence on the oil weight fraction on the whole dispersion for systems with different oleic acid/thymol compositional ratio: (■) 0.84/0.16 and (■) 0.50/0.50.

the dissociation of the species into their ions in solution, and therefore as the concentration of the ionic species increases, in this case with increasing the weight fraction of the oil phase in the whole dispersion increases, the dissociation coefficient of the oleic acid exposed to the aqueous phase must decrease, causing a smaller proportion of ions to remain free in solution. As these free ions are responsible for the electrical conductivity, a decrease in the concentration of these ions leads to a decrease in ionic conductivity.

Based on the results of the conductivity measurements, it is clear that the stabilization of the microemulsions does not only result from the formation of the surfactant film at the droplet/aqueous phase interface, but it is also necessary to take into account the adsorption of part of the oleic acid molecules in the oil phase to this interface. Thus, the oleic acid content in the dispersions appears as a critical parameter for the stabilization of nanodroplet dispersions.

3.4. Fluorescence characterization of nanodroplet dispersions containing thymol

Fluorescence spectroscopy is an analytical technique that is very sensitive to changes in the environment in which molecules are found, so analyzing changes in the fluorescence emission spectrum of a molecule as a result of an encapsulation process is very useful in evaluating encapsulation processes [34]. Here, the changes in the fluorescence properties of thymol as a result of its incorporation into oleic acid nanodroplets stabilized by mixtures of APG and lecithin are studied. Fig. 6 shows the fluorescence spectra, as the fluorescence intensity (I_F) vs. the wavelength (λ), for thymol in solution in oleic acid and for thymol dispersed in oleic acid nanodroplets stabilized by APG and soya lecithin. Fig. 6a shows the difference in the fluorescence emission of thymol as a function of the environment in which it is solubilized, i.e., whether it is solubilized in the oleic acid nanodroplets or simply forms a solution in oleic acid. The changes observed in the fluorescence emission spectrum due to the encapsulation process can be summarized in the following differences. On one hand, the emission maximum appears at different wavelengths, and, on the other hand, the band structure is different, showing one more band in the case where the thymol is solubilized in oleic acid nanodroplets. This last aspect becomes clearer when the spectrum is deconvoluted into Gaussian profile bands, which allows a real representation of the number of transitions involved in the fluorescence spectrum obtained in each case. This analysis is illustrated in Fig. 6b, which shows the deconvolution of the fluorescence spectrum for thymol encapsulated in oleic acid nanodroplets, and in Fig. 6c, which shows the spectrum corresponding to the thymol solution in oleic acid.

The spectrum corresponding to the thymol encapsulated in oleic acid nanodroplets shows the presence of an emission band at λ around 338 nm, together with another band at longer wavelengths (λ = 468 nm) with higher intensity, but a more detailed analysis of the spectrum shows a small shoulder at longer wavelengths, which in the deconvolution appears as a transition at λ around 538 nm. This renders three bands in the case of thymol dispersed in the oleic acid nanodroplets. To identify the possible origin of the bands appearing in the fluorescence spectrum of encapsulated thymol, the spectrum of thymol in solution shown in Fig. 6c can be used as a reference. In contrast to the spectrum of encapsulated thymol, thymol dissolved in oleic acid shows only two bands centered around 380 nm and 440 nm. The appearance of two emission bands can be explained by the formation of thymol clusters, which is consistent with what has been reported in the literature for other aromatic alcohols [35]. Therefore, one of the bands of the thymol spectrum could be attributed to isolated thymol molecules, while the second one could be associated with the formation of clusters of several thymol molecules. Based on the above, it would be possible to discuss the spectrum of encapsulated thymol in relation to thymol in solution.

The encapsulation process causes a slight shift of the emission band appearing at 440 nm in thymol in oleic acid solutions to a higher wavelength (468 nm, bathochromic shift) as a result of the change in

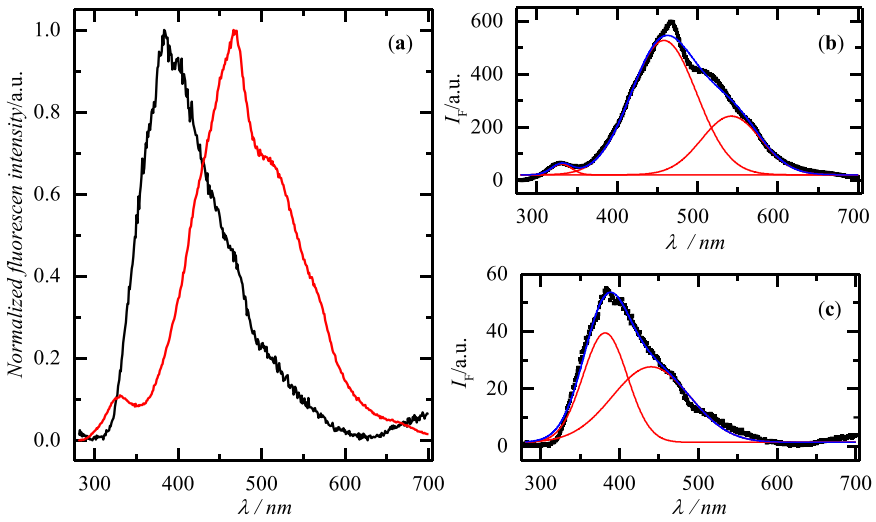

Fig. 6. Fluorescence emission spectra (excitation wavelength 280 nm). (a) Fluorescence spectra, as a representation of the normalized fluorescence intensity against wavelength, corresponding to a solution of thymol in oleic acid with an oleic acid/thymol compositional ratio of 0.5/0.5 (——) and to thymol entrapped in oleic acid nanodroplets (weight fraction of oil phase 0.03, with an oleic acid/thymol compositional ratio of 0.5/0.5) (——). (b) Analysis corresponding to the spectrum of the dispersion of nanodroplets with an oil phase weight fraction of 0.03 and an oleic acid/thymol composition ratio of 0.5/0.5. (c) Analysis corresponding to the spectrum of the solution of thymol in oleic acid with an oleic acid/thymol compositional ratio of 0.5/0.5. In panels (b) and (c), the symbols represent the experimental data, the red lines the obtained bands after deconvolution, and the blue line the theoretical spectrum obtained from the deconvolution.

chemical environment. On the other hand, encapsulation leads to a splitting of the emission band at 380 nm into two different bands, one appearing at a lower wavelength (338 nm, hypsochromic shift) and the other shifting to higher wavelength values (538 nm, bathochromic shift). This splitting phenomenon can be explained by considering that encapsulation leads to the appearance of different chemical microenvironments compared to what occurs in a solution of thymol in oleic acid. This is related to the phenomenon of confinement of the thymol molecules in the nanodroplets, where the thymol can be arranged in different environments. It can therefore be suggested that the three bands that appear in the dispersion spectrum are due to (i) the thymol solubilized near the interfacial region of the nanodroplets (band centered at 338 nm); (ii) the thymol clusters solubilized in the nanodroplet (band centered at 538 nm); and (iii) the individual molecules of the thymol molecules solubilized in the nanodroplets (band centered at 468 nm). Fig. 7 shows the comparison of the emission spectra obtained for dispersions containing a weight fraction of oil phase (oleic acid+thymol) of 0.03 and different oleic acid/thymol compositional ratio.

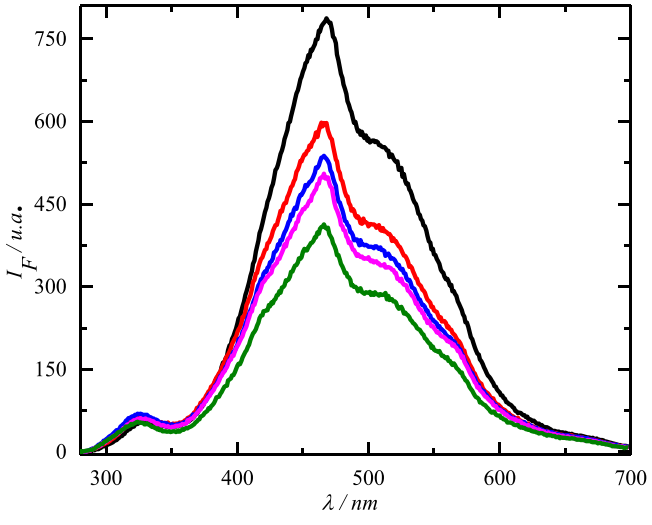

Fig. 7. Comparison of fluorescence spectra for dispersions with an oil phase weight fraction (oleic acid+thymol) of 0.03 and different thymol concentrations, the spectrum with the highest fluorescence intensity corresponds to the sample with the lowest amount of thymol in the oil phase (χ_{thymol} =0.16) and the spectrum with the lowest fluorescence intensity corresponds to the sample with the highest amount of thymol in the oil phase (χ_{thymol}=1.00). Legend (χ_{thymol}): (——) 0.17; (——) 0.50; (——) 0.67; (——) 0.83, and (——) 1.00.

The results corresponding to the modification of the fluorescence spectrum by varying the concentration of thymol in relation to that of oleic acid, keeping the weight fraction of the oil phase constant at 0.03, allow us to observe differences between the emission bands found in the spectrum. The band centered at λ=338 nm is not very sensitive to the thymol concentration and its intensity hardly varies with the thymol weight fraction, whereas the rest of the spectrum is sensitive to the variation in the thymol content dispersed in the oil phase, with a decrease in fluorescence intensity as the thymol concentration increases. This phenomenon can be explained by a self-quenching phenomenon as a result of confinement. As the concentration of encapsulated thymol increases, the crowding of the molecules due to confinement in droplets of similar size is greatly increased. This causes the molecules to be in close proximity to each other, resulting in the formation of aggregates that reduce fluorescence intensity. On the other hand, the band appearing at lower wavelengths hardly changes the emission intensity, suggesting that this transition is associated with solubilized thymol in a region of the microemulsion that does not change significantly with the increase of the total oil volume (oleic acid volume + thymol volume), i.e., the amount of solubilized thymol in this region is very small and therefore its degree of aggregation is very low. This suggests that this band corresponds to thymol solubilized near the droplet interface, probably incorporated into the film formed by the mixture of stabilizing species. Furthermore, the position of this band is consistent with previous studies in which thymol was solubilized in a chemical microenvironment similar to that expected for the interfacial region of the microemulsion [36,37].

The effect of self-quenching by confinement is best understood by analyzing the results in Fig. 8, which shows the dependence of the ratio of the intensities of the emission bands at 468 and 526 nm with respect to the 328 nm band, I_F^{468}/I_F^{328} and I_F^{526}/I_F^{328}, respectively, on the weight fraction of thymol contained in dispersions with a total weight fraction of oil phase of 0.03. The results show that the ratio of band intensities decreases with increasing thymol content in the oil phase, confirming the self-quenching phenomenon discussed above.

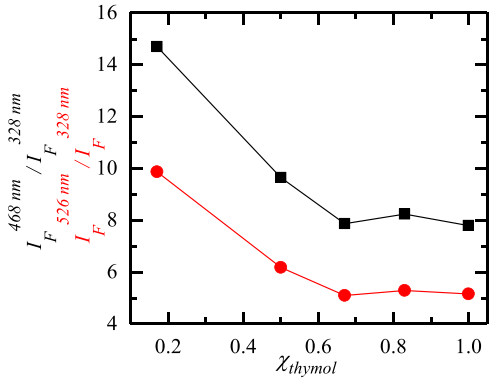

Fig. 8. Dependence on I_F^{468}/I_F^{328} (■) and I_F^{526}/I_F^{328} (●) on the weight fraction of thymol in the oil phase for dispersions with an oil weight fraction of 0.03. The lines are guides for the eyes.

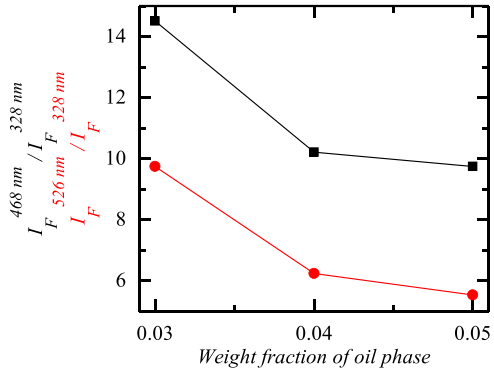

Fig. 9. Dependence on I_F^{468}/I_F^{328} (■) and I_F^{526}/I_F^{328} (●) on the weight fraction of oil phase in the dispersions for dispersions with a thymol fraction in the oil phase χ_{thymol}=0.17. The lines are guides for the eyes.

Another aspect to be investigated is the effect of the total oil phase content on the dispersion. Fig. 9 shows the dependence of the intensity ratio of the emission bands at 468 and 526 nm with respect to the 328 nm band on the weight fraction of the oil phase for dispersions with a fixed weight fraction of thymol (χ_{thymol}=0.17) in the oil phase. The results show a reduction in the intensity ratio for both bands, which again could be understood as a result of the confinement. Thus, although the oleic acid/thymol compositional ratio in the oil phase remains constant as the oil phase content increases, the total concentration of thymol in the droplet increases, which could lead to self-quenching phenomena.

4. Conclusions

A number of methods have been developed for encapsulating thymol and other essential oil compounds, each offering unique advantages. These include polymeric nanocapsules, liposomes, nanofibers, emulsion droplets, or the formation of inclusion complexes with specific molecules. Despite this diversity, oil-in-water emulsion-like dispersions stand out for their remarkable efficiency in encapsulating essential oil compounds while maintaining a straightforward preparation process. This strategic choice not only ensures the protection of thymol, but also guarantees a high level of bioavailability in aqueous media. The simplicity of the emulsion-like dispersion method not only streamlines the encapsulation process, but also promises scalable and practical applications in the formulation of bioactive compounds, highlighting its importance in modern encapsulation techniques. This works has been focused on the ability of oleic acid to favor the dispersion of thymol as nanodroplets, stabilized by a mixture of an alkylpolyglucoside and lecithin, in an aqueous environment.

The results have shown that a careful control of the content and concentration of the oil phase (thymol-oleic acid mixture) plays a crucial role in ensuring optimal thymol dispersion. In fact, these parameters were found to be critical in controlling the stability of the nanodispersions. This results from a complex interplay between the ability of oleic acid to retard thymol crystallization and the maximum amount of oil that can be dispersed as nanodroplets with a given concentration of surfactant. The latter parameter has a decisive influence on the thymol dispersion within the nanodroplets, reducing the maximum amount of thymol that can be included in the dispersion as a result of coalescence and Ostwald ripening phenomena. In fact, the oleic acid content in the dispersions plays a crucial role in stabilizing the dispersions, whereas the increase in thymol content leads to an increase in droplet size, which can trigger destabilization processes. Therefore, finding the most suitable dispersion composition to facilitate thymol solubilization becomes a key challenge. This thymol is unevenly distributed within the droplets, as demonstrated by a fluorescence spectroscopy study, which revealed up to three different chemical environments for its distribution. This investigation is expected to pave the way for novel strategies in the development of efficient platforms to improve the accessibility of biologically relevant, poorly soluble molecules.

CRediT authorship contribution statement

Alejandro Lucia: Writing – review & editing, Supervision, Methodology, Investigation, Conceptualization. **Paula Gutiérrez-González:** Writing – original draft, Visualization, Software, Methodology, Investigation, Formal analysis, Data curation. **Laura Fernández-Peña:** Writing – review & editing, Visualization, Validation, Supervision, Software, Methodology, Investigation, Formal analysis, Data curation. **Francisco Ortega:** Writing – review & editing, Validation, Supervision, Resources, Project administration, Investigation, Funding acquisition. **Ramón G. Rubio:** Writing – review & editing, Validation, Supervision, Resources, Project administration, Investigation, Funding acquisition, Conceptualization. **Eduardo Guzman:** Writing – review & editing, Writing – original draft, Validation, Supervision, Project administration, Methodology, Investigation, Funding acquisition, Data curation, Conceptualization.

Declaration of Competing Interest

The authors declare that they have no known competing financial interests or personal relationships that could have appeared to influence the work reported in this paper.

Data Availability

Data will be made available on request.

Acknowledgements

This work was partly funded by MCIN (Spain) under grant PID2019-106557GB-C21, and by the E.U. in the framework of the European Innovative Training Network-Marie Sklodowska-Curie Action Nano-PaInt (grant agreement 955612).

References

[1] S. Sharma, L. Mulrey, M. Byrne, A.K. Jaiswal, S. Jaiswal, Encapsulation of essential oils in nanocarriers for active food packaging, Foods 11 (2022) 2337, https://doi.org/10.3390/foods11152337.

[2] A. Lucia, E. Guzmán, Emulsions containing essential oils, their components or volatile semiochemicals as promising tools for insect pest and pathogen management, Adv. Colloid Interface Scie. 287 (2021) 102330, https://doi.org/10.1016/j.cis.2020.102330.

[3] S. Panda, S. Sahoo, K. Tripathy, Y.D. Singh, M.K. Sarma, P.J. Babu, M.C. Singh, Essential oils and their pharmacotherapeutics applications in human diseases, Adv. Tradit. Med. 22 (2022) 1–15, https://doi.org/10.1007/s13596-020-00477-z.
[4] W. Dhifi, S. Bellili, S. Jazi, N. Bahloul, W. Mnif, Essential oils' chemical characterization and investigation of some biological activities: a critical review, Medicines 3 (2016) 25, https://doi.org/10.3390/medicines3040025.
[5] E. Guzmán, A. Lucia, Essential oils and their individual components in cosmetic products, Cosmetics 8 (2021) 114, https://doi.org/10.3390/cosmetics8040114.
[6] A.R. Mukurumbira, R.A. Shellie, R. Keast, E.A. Palombo, S.R. Jadhav, Encapsulation of essential oils and their application in antimicrobial active packaging, Food Control 136 (2022) 108883, https://doi.org/10.1016/j.foodcont.2022.108883.
[7] G.G. Lenetha, A. Brief, Overview on the essential oils' encapsulation with biodegradable, Polym., Nat. Volatiles Essent. Oils 9 (2022) 415–422.
[8] D.R. Reis, A. Ambrosi, M.Di Luccio, Encapsulated essential oils: a perspective in food preservation, Future Foods 5 (2022) 100126, https://doi.org/10.1016/j.fufo.2022.100126.
[9] H. A. Shaaban, A. Farouk, Encapsulation of Essential Oils and Their Use in Food Applications, in: Mozaniel Santana De Oliveira, Eloisa Helena De Aguiar Andrade (Eds.), Essential Oils, Intech Open, London, UK, 2022. https://doi.org/10.5772/intechopen.103147.
[10] C. Maes, S. Bouquillon, M.L. Fauconnier, Encapsulation of essential oils for the development of biosourced pesticides with controlled release: a review, Molecules 24 (2019) 2539, https://doi.org/10.3390/molecules24142539.
[11] V.I. Sousa, J.F. Parente, J.F. Marques, M.A. Forte, C.J. Tavares, Microencapsulation of essential oils: a review, Polym. (Basel) 14 (2022) 1730, https://doi.org/10.3390/polym14091730.
[12] D.R. Reis, A. Ambrosi, M.Di Luccio, Encapsulated essential oils: a perspective in food preservation, Future Foods 5 (2022) 100126, https://doi.org/10.1016/j.fufo.2022.100126.
[13] Z. Aksoylu, P. Günç Ergönül, A review on encapsulation of oils, Celal Bayar Üniversitesi Fen. Bilim. Derg. 13 (2017) 293–309, https://doi.org/10.18466/cbayarfbe.313358.
[14] Z. Dajic Stevanovic, E. Sieniawska, K. Glowniak, N. Obradovic, I. Pajic-Lijakovic, Natural macromolecules as carriers for essential oils: from extraction to biomedical application, Front. Bioeng. Biotechnol. 8 (2020) 00563, https://doi.org/10.3389/fbioe.2020.00563.
[15] R. Pavela, G. Benelli, L. Pavoni, G. Bonacucina, M. Cespi, K. Cianfaglione, I. Bajalan, M.R. Morshedloo, G. Lupidi, D. Romano, A. Canale, F. Maggi, Microemulsions for delivery of Apiaceae essential oils—towards highly effective and eco-friendly mosquito larvicides? Ind. Crop Prod. 129 (2019) 631–640, https://doi.org/10.1016/j.indcrop.2018.11.073.
[16] T.N. Barradas, K.G. de Holanda e Silva, Nanoemulsions as optimized vehicles for essential oils (Cham), in: A. Saneja, A.K. Panda, E. Lichtfouse (Eds.), Sustainable Agriculture Reviews: Pharmaceutical Technology for Natural Products Delivery, Springer, Switzerland, 2020, pp. 115–167, https://doi.org/10.1007/978-3-030-41842-7_4 (Cham).
[17] L. Pavoni, D.R. Perinelli, G. Bonacucina, M. Cespi, G.F. Palmieri, An overview of micro- and nanoemulsions as vehicles for essential oils: formulation, preparation and stability, Nanomaterials 10 (2020) 135, https://doi.org/10.3390/nano10010135.
[18] M.F. Nagoor Meeran, H. Javed, H. Al Taee, S. Azimullah, S.K. Ojha, Pharmacological properties and molecular mechanisms of thymol: prospects for its therapeutic potential and pharmaceutical development, Front. Pharmacol. 8 (2017) 380, https://doi.org/10.3389/fphar.2017.00380.
[19] D. Villanueva Bermejo, I. Angelov, G. Vicente, R.P. Stateva, M. Rodriguez García-Risco, G. Reglero, E. Ibañez, T. Fornari, Extraction of thymol from different varieties of thyme plants using green solvents, J. Sci. Food Agric. 95 (2015) 2901–2907, https://doi.org/10.1002/jsfa.7031.
[20] P. Zhu, Y. Chen, J. Fang, Z. Wang, C. Xie, B. Hou, W. Chen, F. Xu, Solubility and solution thermodynamics of thymol in six pure organic solvents, J. Chem. Therm. 92 (2016) 198–206, https://doi.org/10.1016/j.jct.2015.09.010.
[21] J. Yammine, A. Gharsallaoui, A. Fadel, L. Karam, A. Ismail, N.-E. Chihib, Encapsulation of carvacrol and thymol for a persistent removal of Listeria innocua biofilms, J. Drug Deliv. Sci. Technol. 84 (2023) 104443, https://doi.org/10.1016/j.jddst.2023.104443.
[22] K. Shlosman, D.M. Rein, R. Shemesh, N. Koifman, A. Caspi, Y. Cohen, Encapsulation of thymol and eugenol essential oils using unmodified cellulose: preparation and characterization, Polym. (Basel) 15 (2022) 95, https://doi.org/10.3390/polym15010095.
[23] J. Zhou, L. Kong, Encapsulation and retention profile of thymol in the preformed "empty" V-type starch inclusion complex, Food Front 4 (2023) 902–910, https://doi.org/10.1002/fft2.222.
[24] M.A. Ruiz, J.L. Arias, V. Gallardo, Skin creams made with olive oil, in: V.R. Preedy, R.R. Watson (Eds.), Olives and Olive Oil in Health and Disease Prevention, Academic Press, Cambridge, MA, USA, 2010: pp. 1133–1141. https://doi.org/10.1016/B978-0-12-374420-3.00124-8.
[25] T.M. Isailović, M.N. Todosijević, S.M. Đorđević, S.D. Savić, Natural Surfactants-Based Micro/Nanoemulsion Systems for NSAIDs—Practical Formulation Approach, Physicochemical and Biopharmaceutical Characteristics/Performances, in: B. Čalija (Ed.), Microsized and Nanosized Carriers for Nonsteroidal Anti-Inflammatory Drugs, Academic Press, Cambridge, MA, USA, 2017: pp. 179–217. https://doi.org/10.1016/B978-0-12-804017-1.00007-8.
[26] M. Wang, W. Yan, Y. Zhou, L. Fan, Y. Liu, J. Li, Progress in the application of lecithins in water-in-oil emulsions, Trends Food Sci. Technol. 118 (2021) 388–398, https://doi.org/10.1016/j.tifs.2021.10.019.
[27] I. Pantelic, M. Lukic, R. Daniels, E. Karls, S. Savic, Alkyl Polyglucoside-based delivery systems: In vitro/in vivo skin absorption assessment (Sawston), in: I. Pantelic (Ed.), Alkyl Polyglucosides: From Natural-Origin Surfactants to Prospective Delivery Systems, Woodhead Publishing, UK, 2014, pp. 107–134, https://doi.org/10.1533/9781908818775.107 (Sawston).
[28] L. Fernández-Peña, S. Gutiérrez-Muro, E. Guzmán, A. Lucia, F. Ortega, R. G. Rubio, Oil-In-water microemulsions for thymol solubilization, Colloids Interfaces 3 (2019) 64, https://doi.org/10.3390/colloids3040064.
[29] A. Lucia, P.G. Argudo, E. Guzmán, R.G. Rubio, F. Ortega, Formation of surfactant free microemulsions in the ternary system water/eugenol/ethanol, Colloids Surf. A Physicochem Eng. Asp. 521 (2017), https://doi.org/10.1016/j.colsurfa.2016.04.062.
[30] A. Lucia, A.C. Toloza, E. Guzmán, F. Ortega, R.G. Rubio, Novel polymeric micelles for insect pest control: encapsulation of essential oil monoterpenes inside a triblock copolymer shell for head lice control, PeerJ 2017 (2017), https://doi.org/10.7717/peerj.3171.
[31] Huanbo Wang, Yu Jun, Xue Xiao, Dan Jin, Nan-Jing Zhao, Gao-Fang Yin, Li-Quan Guo, Wen-Qing Liu, Excitation-emission fluorescence characterization study of the three phenolic compounds, Spectrosc. Spect. Anal. 30 (30AD) 1271–1274.
[32] A. Sedaghat Doost, J. Van Camp, K. Dewettinck, P. Van der Meeren, Production of thymol nanoemulsions stabilized using Quillaja Saponin as a biosurfactant: antioxidant activity enhancement, Food Chem. 293 (2019) 134–143, https://doi.org/10.1016/j.foodchem.2019.04.090.
[33] B.J. Berne, R. Pecora. Dynamic Light Scattering: With Applications to Chemistry, Biology, and Physics, John Wiley & Sons, New York, NY, USA, 2003.
[34] M. Sauer, J. Hofkens, J. Enderlein, Weinheim, Germany. Handbook of Fluorescence Spectroscopy and Imaging, Wiley, 2011, https://doi.org/10.1002/9783527633500.
[35] O.N. Tchaikovskaya, I.V. Sokolova, R.T. Kuznetsova, V.A. Swetlitchnyi, T. N. Kopylova, G.V. Mayer, Fluorescence investigations of phenol phototransformation in aqueous solutions, J. Fluor. 10 (2000) 403–408, https://doi.org/10.1023/A:1009486615346.
[36] A. Bose, P. Sengupta, U. Pal, S. Senapati, Mohd Ahsan, S. Roy, U. Das, K. Sen, Encapsulation of Thymol in cyclodextrin nano-cavities: a multi spectroscopic and theoretical study, Spectrochim. Acta A: Mol. Biomol. Spectrosc. 208 (2019) 339–348, https://doi.org/10.1016/j.saa.2018.10.011.
[37] K. Pan, H. Chen, P.M. Davidson, Q. Zhong, Thymol nanoencapsulated by sodium caseinate: physical and antilisterial properties, J. Agric. Food Chem. 62 (2014) 1649–1657, https://doi.org/10.1021/jf4055402.